*Progress In Electromagnetics Research M, Vol. 59, 135–146, 2017*

# Inverse Scattering of a Conducting Cylinder in Free Space by Modified Fireworks Algorithm

**Kun-Chou Lee***

**Abstract**—In this paper, the inverse scattering of a conducting cylinder is given by modified fireworks algorithm. Initially, the direct scattering is formulated as an integral equation, which contains the target shape function. The scattering integral equation is then solved by the moment method. To achieve image reconstruction, the target shape function is expanded as a Fourier series. The inverse scattering is transformed into a nonlinear optimization problem. The variables are Fourier series coefficients of the target shape function. The objective function is defined by comparing the scattered electric fields of guessed and true shapes. This nonlinear optimization problem is then optimized by our modified fireworks algorithm. The fireworks algorithm is a novel swarm intelligence algorithm for global optimization. It is inspired by practical fireworks explosion. In this paper, it is suitably modified so that it can treat the inverse scattering problem with fast convergence. Numerical results show that the inverse scattering based on our modified fireworks algorithm can accurately reconstruct the target shape with fast convergence.

## 1. INTRODUCTION

Inverse scattering plays a very important role in radar, remote sensing, non-destructive testing, etc. For a conducting target, the inverse scattering techniques are basically divided into two categories. The first category is based on the physical optics approximation and discrete Fourier transformation, such as [1–5]. The main advantage of this category is that the computation is very efficient. However, the inverse scattering technique of this category is limited to only a convex target with the smooth surface The second category is to solve nonlinear scattering integral equations directly by numerical methods, such as [6–10]. The main advantage of this category is that there is no limitation on the target shape. However, the computation is time-consuming and even difficult due to the nonlinearity and ill-posed problems. In [11], the technique of the second category is modified and further transformed into a nonlinear optimization problem. Thus the inverse scattering becomes a nonlinear optimization problem. This will make the inverse scattering scheme clear and easy since numerical techniques for solving nonlinear integral equations have been replaced by optimization algorithms

In recent years, swarm intelligence has become important in nonlinear optimization. Such optimization techniques are often inspired by some intelligent colony behaviors in nature. In particular, the fireworks algorithm [12] mimics the explosion process of fireworks, and is an important technique of swarm intelligence optimization. It is inspired by the emergent swarm behavior of fireworks. This nonlinear optimization algorithm is implemented by simulating the explosion process of fireworks. In terms of both optimization accuracy and convergence speed it has been proved to outperform the particle swarm optimization algorithm, which is a well-known nature inspiration optimization algorithm [12, 13]. This motivates us to apply the fireworks algorithm to inverse scattering problem.

*Received 11 June 2017, Accepted 8 August 2017, Scheduled 15 August 2017*

* Corresponding author: Kun-Chou Lee (kclee@mail.ncku.edu.tw).

The author is with the Department of Systems and Naval Mechatronic Engineering, National Cheng-Kung University, Tainan 701, Taiwan.

In this paper, the firework algorithm [12] is modified and then applied to inverse scattering of a conducting cylinder in free space Based on the scattering integral equation [14] and moment method [15], the inverse scattering is first transformed into a nonlinear optimization. The variables are the Fourier series coefficients [16]. The objective function is defined by comparing scattered electric fields from the guessed and true shapes, respectively. Numerical results show that the target shape reconstructed by the fireworks algorithm is very accurate and the convergence is fast.

The remainder of this paper is organized as follows. Section 2 describes the direct scattering. Section 3 describes the inverse scattering. Section 4 gives the modified fireworks algorithm. Numerical results are given in Section 5. Finally, conclusions are given in Section 6.

## 2. DIRECT SCATTERING

For simplicity without loss of generality, this study considers only two-dimensional problems. Consider a perfectly conducting cylinder in free space illuminated by an incident plane wave

$$\bar{E}_i = E_i\hat{z} = \exp\{-jk(x\sin\phi_i + y\cos\phi_i)\}\hat{z}, \tag{1}$$

as shown in Fig. 1. Note that the time harmonic factor $\exp(j\omega t)$ is omitted. In Eq. (1) and Fig. 1, $k$ is the wavenumber, and $\phi_i$ is an angle representing the incident direction. The target cylinder is infinitely extended in $\pm\hat{z}$ directions. Let $(\rho, \phi)$ denote the polar coordinates in $x$-$y$ plane. For any point on the target boundary, its polar coordinates are characterized by a shape function $\rho = h(\phi)$. According to [14], the scattered electric field at position $(xy)$ is also $\hat{z}$-polarized and can be expressed as

$$\begin{aligned} E_S(x,y) \;=\; & -\frac{k\eta_0}{4}\int_0^{2\pi} H_0^{(2)}\left(k\sqrt{[x-h(\phi')\cos\phi']^2 + \;[y-h(\phi')\sin\phi']^2}\right) \\ & \sqrt{[h(\phi')]^2 + \;[h'(\phi')]^2}J_S(\phi')d\phi'. \end{aligned} \tag{2}$$

In Eq. (2), $\eta_0 = 120\pi$ is the intrinsic impedance of free space, $H_0^{(2)}(\cdot)$ the zero-order Hankel function of the second kind, and $J_S(\cdot)$ the surface current density. Note that the mark, prime, represents the current source. According to the electromagnetic boundary condition, the total electric field is zero on the target boundary. Thus for any point with polar coordinates $(h(\phi), \phi)$ on the target boundary, we

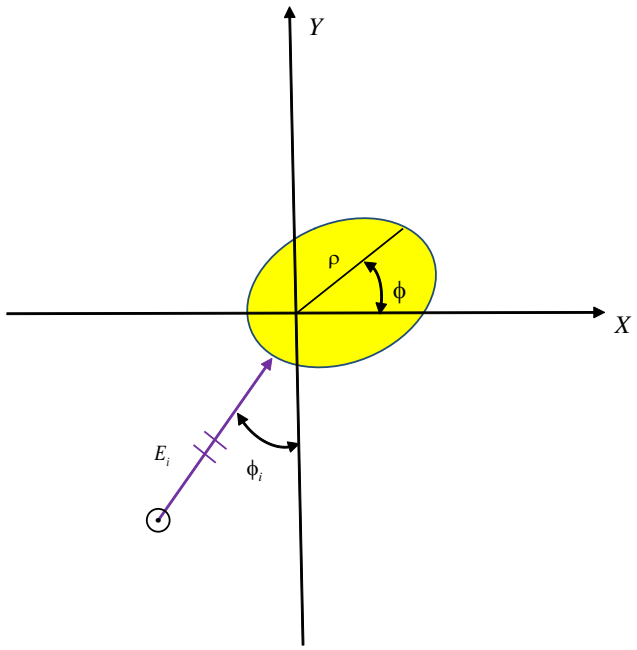


**Figure 1.** Geometry of a cylinder in free space illuminated by an incident plane wave $\bar{E}_i = E_i\hat{z}$.

have $E_i = -E_S$, i.e.,

$$E_i(h(\phi),\phi) = \frac{k\eta_0}{4}\int_0^{2\pi} H_0^{(2)}\left(k\sqrt{[h(\phi)]^2 + [h(\phi')]^2 - 2h(\phi)h(\phi')\cos(\phi-\phi')}\right) \sqrt{[h(\phi')]^2 + [h'(\phi')]^2}J_S(\phi')d\phi'. \tag{3}$$

To obtain scattered electric field $E_S$, the surface current density $J_S(\cdot)$ should be determined. By using moment methods [15], $J_S(\cdot)$ is expanded as

$$J_S(\phi') = \sum_{n=1}^{N_B} I_n B_n(\phi'), \tag{4}$$

where $I_1, I_2, \ldots, I_{N_B}$ are unknown coefficients and $B_1(\cdot), B_2(\cdot), \ldots, B_{N_B}(\cdot)$ are known basis functions, which are

$$B_n(\phi') = \begin{cases} 1, & (n-1)\cdot 2\pi/N_B \le \phi' < n\cdot 2\pi/N_B \\ 0, & \text{otherwise.} \end{cases} \tag{5}$$

As unknown coefficients $I_1, I_2, \ldots, I_{N_B}$ are determined, $J_S(\cdot)$ are obtained from Eq. (4). Substituting Eqs. (4) and (5) into Eq. (3), we have

$$\frac{k\eta_0}{4}\sum_{n=1}^{N_B}\int_{(n-1)\cdot 2\pi/N_B}^{n\cdot 2\pi/N_B} I_n\left\{H_0^{(2)}\left(k\sqrt{[h(\phi)]^2 + [h(\phi')]^2 - 2h(\phi)h(\phi')\cos(\phi-\phi')}\right) \sqrt{[h(\phi')]^2 + [h'(\phi')]^2}d\phi'\right\} = E_i(h(\phi),\phi) \tag{6}$$

for any point with polar coordinates $(h(\phi), \phi)$ on the target boundary. By setting $\phi = \phi_m = (m-0.5)\cdot 2\pi/N_B$, $m = 1, 2, \ldots, N_B$ in Eq. (6), we obtain $N_B$ simultaneous equations as

$$\sum_{n=1}^{N_B} Z_{mn} I_n = V_m, \quad m = 1, 2, \ldots, N_B, \tag{7}$$

where

$$Z_{mn} = \frac{k\eta_0}{4}\int_{(n-1)\cdot 2\pi/N_B}^{n\cdot 2\pi/N_B} H_0^{(2)}\left(k\sqrt{[h(\phi_m)]^2 + [h(\phi')]^2 - 2h(\phi_m)h(\phi')\cos(\phi_m-\phi')}\right) \sqrt{[h(\phi')]^2 + [h'(\phi')]^2}d\phi' \tag{8}$$

and

$$V_m = \exp\{-jk[h(\phi_m)\cos\phi_m \sin\phi_i + h(\phi_m)\sin\phi_m\cos\phi_i]\}. \tag{9}$$

From Eqs. (7)–(9), $I_n$ $(n = 1, 2, \ldots, N_B)$ can be obtained by solving the simultaneous equations. The scattered field $E_S(x, y)$ at any position $(xy)$ can be obtained by substituting $I_n$ $(n = 1, 2, \ldots, N_B)$ into Eq. (4) and then into Eq. (2). The result is

$$E_S(x,y) = -\frac{k\eta_0}{4}\sum_{n=1}^{N_B} I_n\int_{(n-1)\cdot 2\pi/N_B}^{n\cdot 2\pi/N_B} H_0^{(2)}\left(k\sqrt{[x-h(\phi')\cos\phi']^2 + [y-h(\phi')\sin\phi']^2}\right) \sqrt{[h(\phi')]^2 + [h'(\phi')]^2}d\phi'. \tag{10}$$

## 3. INVERSE SCATTERING

Inverse scattering means to reconstruct the target shape from scattered fields. For convenience, the target shape function is expanded into a Fourier series as

$$\rho = h(\phi) = C_0 + \sum_{n=1}^{N_S}[C_n\cos(n\phi) + S_n\sin(n\phi)], \tag{11}$$

where $N_S$ is the maximum number of harmonics. $C_n$ $(n = 0, \ldots, N_S)$ and $S_n$ $(n = 1, \ldots, N_S)$ are unknown real coefficients. As the target shape is non-canonical and complex, the expansion of Eq. (11) may be inadequate. In such a case, the cubic spline interpolation [17] may be utilized instead to expand the target shape. The inverse scattering problem becomes to determine $C_n$ $(n = 0, \ldots, N_S)$ and $S_n$ $(n = 1, \ldots, N_S)$ from collection of scattered fields. To achieve adequate features of scattering mechanisms, the target is illuminated by incident wave from $N_I$ different incident directions of $\phi_i$. For each incidence, the scattered electric fields are collected at $N_L$ different locations. The inverse scattering problem becomes to find optimum values of $C_n$ $(n = 0, \ldots, N_S)$ and $S_n$ $(n = 1, \ldots, N_S)$ that minimize the objective function

$$f = \sum_{i=1}^{N_I} \sum_{l=1}^{N_L} \left( \left| E_{i,l}^{guess} - E_{i,l}^{true} \right| \Big/ \left| E_{i,l}^{true} \right| \right), \tag{12}$$

where $E_{i,l}^{guess}$ and $E_{i,l}^{true}$ are scattered electric fields from the guessed and true shapes of the target, respectively. The subscripts represent the $l$-th location of the $i$-th incidence. So far, the inverse scattering has been transformed into a nonlinear optimization problem. The variables are $C_n$ $(n = 0, \ldots, N_S)$ and $S_n$ $(n = 1, \ldots, N_S)$ in Eq. (11). As the objective function of Eq. (12) is minimized, the target shape function of Eq. (11) is reconstructed. In this paper, the minimization of Eq. (12) is implemented by the modified fireworks algorithm [12], as given in the next section.

## 4. MODIFIED BY FIREWORKS ALGORITHM

In this study, we modify the fireworks algorithm in [12] to implement the minimization of Eq. (12). Note that the procedures of fireworks algorithm in this study are somewhat different from those of reference [12]. We make some modifications by experiences so that they can converge well in our inverse scattering problem. The idea of fireworks algorithm optimization is from practical fireworks and their sparks [12]. When a firework is well manufactured, numerous sparks are generated and centralize the explosion center. On the contrary for a bad firework explosion, quite few sparks are generated and sparks scatter far from the explosion center. These two types of fireworks explosion are shown in Fig. 2.

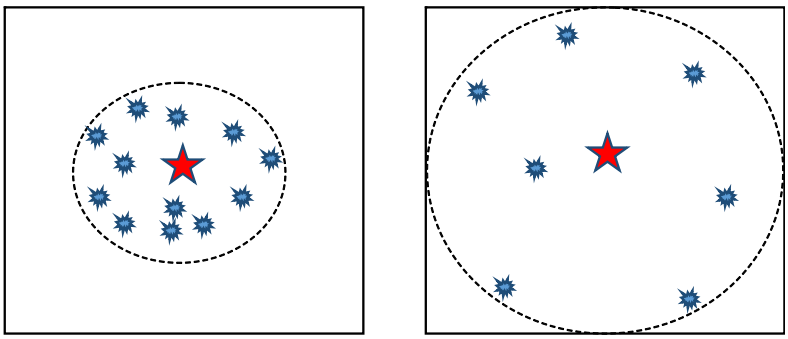


**Figure 2.** Explosions of (a) good and (b) bad fireworks.

Assume that the problem is

$$\text{Minimizing } f(\bar{r}) \text{ for } \bar{r} = (x_1, x_2, \ldots, x_D), \tag{13}$$

under the constraint

$$\alpha_d \le x_d \le \beta_d, \quad d = 1, 2, \ldots, D. \tag{14}$$

In Eq. (13), $\bar{r}$ is the location of a firework in potential space, and $f(\bar{r})$ is its objective function. In Eq. (14), $\alpha_d$ and $\beta_d$ denote the lower and upper bounds of $x_d$, $d = 1, 2, \ldots, D$, respectively. In Eqs. (13) and (14), $D$ is the number of dimensions for the location in potential space. A flowchart of the modified fireworks algorithm is given in Fig. 3 Detailed procedures are given in the following.

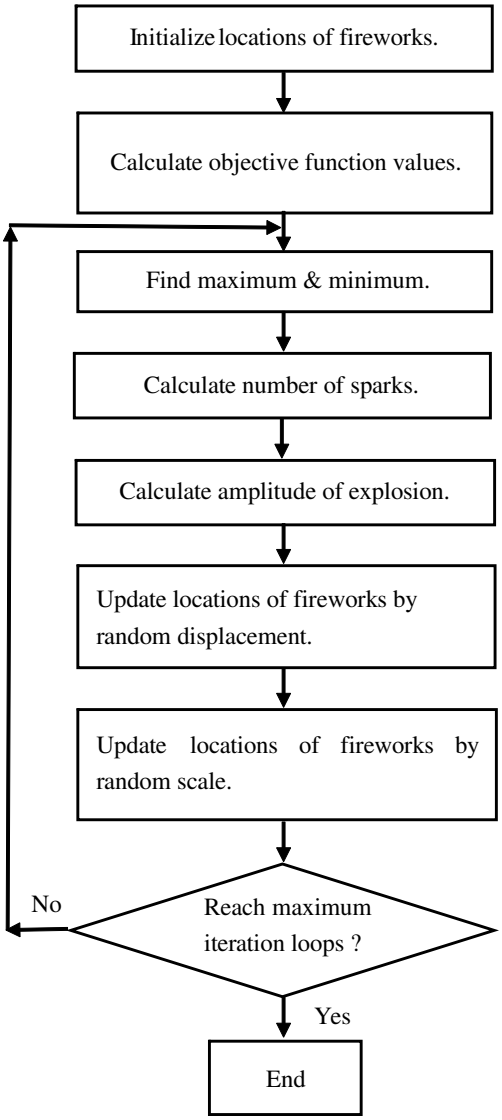


**Figure 3.** The flowchart of modified fireworks algorithm.

***Step-1:** Initialize the locations of fireworks. Assume that there are $N$ fireworks in total. Their initial locations are selected randomly and denoted as $\bar{r}_1, \bar{r}_2 \ldots, \bar{r}_N$.

***Step-2:** Calculate the objective function values $f(\bar{r}_i)$, $i = 1, 2, \ldots, N$, for the $N$ fireworks.

***Step-3:** Find the maximum ($y_{\max}$) and minimum ($y_{\min}$) for objective function values of the $N$ fireworks.

***Step-4:** Calculate the number of sparks for each firework. The number of sparks generated by the $i$-th firework (located at $\bar{r}_i$) is given as

$$S_i = M_S \cdot \frac{y_{\max} - f(\bar{r}_i) + \xi}{\sum_{i=1}^{N} [y_{\max} - f(\bar{r}_i)] + \xi}, \quad i = 1, 2, \ldots, N. \tag{15}$$

where $M_S$ is a parameter controlling the total number of sparks generated by the $N$ fireworks. In Eq. (15), $\xi$ is a constant to avoid zero division error. Note that Eq. (15) means that a better firework, i.e., with smaller $f(\bar{r}_i)$, generates more sparks. On the contrary, a worse firework, i.e.,

with larger $f(\bar{r}_i)$, generates less sparks. Bounds of $S_i$, $i = 1, 2, \ldots, N$, are chosen as

$$S_i = \begin{cases} \text{round}(a \cdot M), & S_i < a \cdot M \\ \text{round}(b \cdot M), & S_i > b \cdot M \\ \text{round}(S_i), & \text{otherwise} \end{cases}, \tag{16}$$

where $a$ and $b$ are constants, and $0 < a < b < 1$.

***Step-5:** Calculate the amplitude of explosion. The amplitude of explosion is given as

$$A_i = A \cdot \frac{f(\bar{r}_i) - y_{\min} + \xi}{\sum_{i=1}^{N} [f(\bar{r}_i) - y_{\min}] + \xi}, \quad i = 1, 2, \ldots, N. \tag{17}$$

where $A$ denotes the maximum explosion amplitude. Note that Eq. (17) means that a better firework, i.e., with smaller $f(\bar{r}_i)$, has a smaller explosion amplitude. On the contrary, a worse firework, i.e., with larger $f(\bar{r}_i)$, has a larger explosion amplitude. Therefore, Eq. (17) hints that a good firework generates sparks near the explosion center, whereas a bad firework generates sparks scattering far from the explosion center.

***Step-6:** Update locations of fireworks by random displacement. Assume that the $i$-th firework ($i = 1, 2, \ldots, N$) is located at $\bar{r}_i = (x_{i,1}, x_{i,2}, \ldots, x_{i,D})$. Its spark has random displacement with respect to the firework. The spark location $\bar{r}_S = (x_{S,1}, \ldots, x_{S,d}, \ldots, x_{S,D})$ is given as

$$x_{S,d} = x_{i,d} + A_i \cdot \text{rand}(-1,\ 1), \quad d = 1, 2, \ldots, D, \tag{18}$$

where $rand(-1, 1)$ is a random number between $-1$ and 1. Next calculate the objective function value $f(\bar{r}_S)$. If $f(\bar{r}_S)$ is less than $f(\bar{r}_i)$, $\bar{r}_i$ is replaced by $\bar{r}_S$. The procedure of Eq. (18) together with check of the objective function value will be repeated $S_i$ times, since there are $S_i$ fireworks generated by the $i$-th firework.

***Step-7:** Update locations of fireworks by random scale. The $i$-th firework ($i = 1, 2, \ldots, N$) generates a specific spark. Its location $\bar{r}_S = (x_{S,1}, \ldots, x_{S,d}, \ldots, x_{S,D})$ is given as

$$x_{S,d} = x_{i,d} \cdot Gaussian(1, 1), \quad d = 1, 2, \ldots, D, \tag{19}$$

where $Gaussian(1, 1)$ is a Gaussian distribution random number with mean 1 and standard deviation 1. Next calculate the objective function value $f(\bar{r}_S)$. If $f(\bar{r}_S)$ is less than $f(\bar{r}_i)$, $\bar{r}_i$ is replaced by $\bar{r}_S$. The procedure of Eq. (19) together with check of the objective function value will be repeated $M_G$ times, i.e., there are $M_G$ specific fireworks generated by the $i$-th firework.

***Step-8:** Go to *Step-3* until the number of iteration loops reaches a pre-specified threshold, i.e., maximum iteration loops.

In this study, we utilize the above modified fireworks algorithm to achieve inverse scattering. Components of the firework location $\bar{r} = (x_1, x_2, \ldots, x_D)$ of Eq. (13) represents Fourier series coefficients of Eq. (11), i.e.,

$$\bar{r} = (x_1,\ x_2,\ \ldots,\ x_D) = (C_0,\ C_1,\ \ldots,\ C_{N_S},\ S_1,\ \ldots,\ S_{N_S}). \tag{20}$$

The objective function of Eq. (13) is defined as Eq. (12). Following the above iteration procedures of our modified fireworks algorithm, the optimum Fourier coefficients of the target shape can be obtained. The target shape is then reconstructed by Eq. (11).

## 5. NUMERICAL RESULTS

In this section, numerical examples are given to illustrate the above image reconstruction algorithm. Consider a perfectly conducting cylinder in free space illuminated by a plane wave of Eq. (1), as shown in Fig. 1. The frequency of the incident wave is 3 GHz. The incident wave direction $\phi_i$ is chosen as 0°, 120°, and 240°, respectively. For each incidence, scattered electric fields are collected in eight directions, which are $\phi$ = 0°, 45°, 90°, 135°, ..., and 315°, respectively. That is, we have $N_I = 3$ and $N_L = 8$ in Eq. (12). The distance between each receiver and the target is chosen as 12 m. Note

that the scattered electric field is calculated by Eq. (10), which is suitable for both near and far fields. Therefore, the choice of distance between a receiver and the target is not important. This study focuses on numerical simulation for verifying that the fireworks algorithm can implement inverse scattering. The basic consideration of the above antenna array arrangement is to capture features from all aspects of the target. In the future, the optimal synthesis of an antenna array may be considered, as those given in reference [18]. The $N_S$ in Eq. (11) is set to be 4, i.e., the target shape is characterized by a Fourier series with $9(= 2 \times 4 + 1)$ terms. Although the increase of $N_S$ improves the discrimination of target shape, it will also lead to time-consuming computation. The optimal value of $N_S$ depends on the degrees of freedom of scattered fields [19, 20]. However, this is not the focus of this study. This study focuses on how the fireworks algorithm is embedded into the inverse scattering scheme. Note that the goal of inverse scattering is to determine these 9 Fourier series coefficients and then reconstruct the target shape as Eq. (11). The problem is first transformed into a nonlinear optimization problem as Eq. (12) and then optimized by the modified fireworks algorithm as Section 4. In our modified fireworks algorithm, the number of fireworks is chosen as $N = 10$. The location of each firework has 9 dimensions ($D = 9$) to represent the 9-term Fourier series coefficients of the target shape function in Eq. (11). In *Step-1* of Section 4, the initial guess of each firework location is generated by an uniformly random number within a fixed range The $M_S$ of Eq. (15), which is a parameter controlling the total number of sparks is chosen as $M_S = 100$. The $\xi$ of Eqs. (15) and (17), which is a constant to avoid zero division error, is chosen as $\xi = 0.1$. The $a$ and $b$ of Eq. (16) are chosen as $a = 0.04$ and $b = 0.8$, respectively. The maximum explosion amplitude$A$ in Eq. (17) is set to be 10. The number of specific fireworks in Step-7 of Section 4 is chosen as $M_G = 5$.

In the first example, the target shape function is given as $h(\phi) = 0.4 + 0.1\cos(\phi) + 0.03\cos(2\phi) + 0.05\sin(\phi) + 0.02\sin(3\phi)$, which is convex as shown in Fig. 4. Following the above inverse scattering procedures, the reconstructed target shape of different iteration loops is plotted in Fig. 4. The shape error is defined as

$$Shape\ Error = \frac{1}{M_{ang}} \sum_{m=1}^{M_{ang}} \frac{\left|\rho^{guess}(\phi_m) - \rho^{true}(\phi_m)\right|}{\left|\rho^{true}(\phi_m)\right|}, \tag{21}$$

where $\rho^{guess}(\cdot)$ and $\rho^{true}(\cdot)$ represent the radius in polar coordinates for guessed and true shapes, respectively. The $\phi_m$ $(m = 1, 2, \ldots, M_{ang})$ denotes the sampling angle. In this study, $\phi_m$ is chosen as 1, 2, ..., 360, i.e., $M_{ang} = 360$. Fig. 5 shows the shape error with respective to iteration loops. Fig. 6

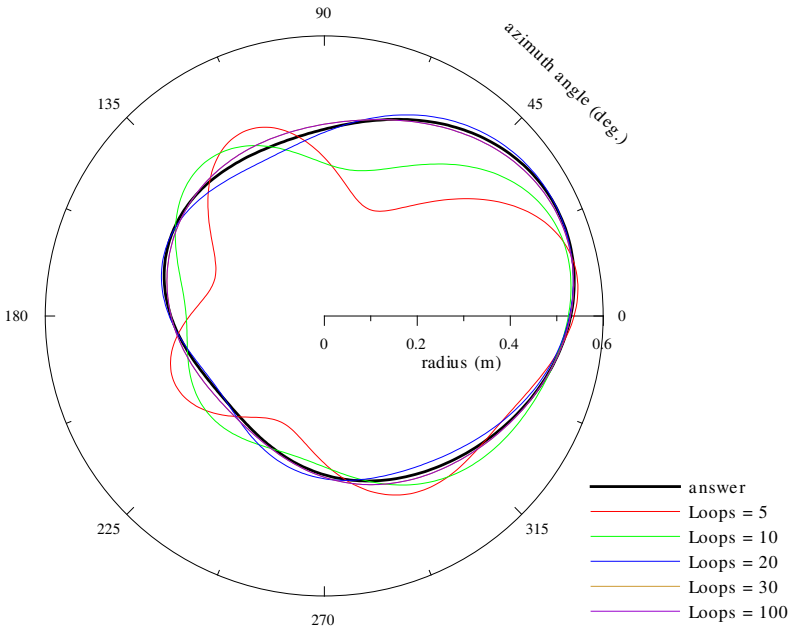


**Figure 4.** The reconstructed target shape of the first example.

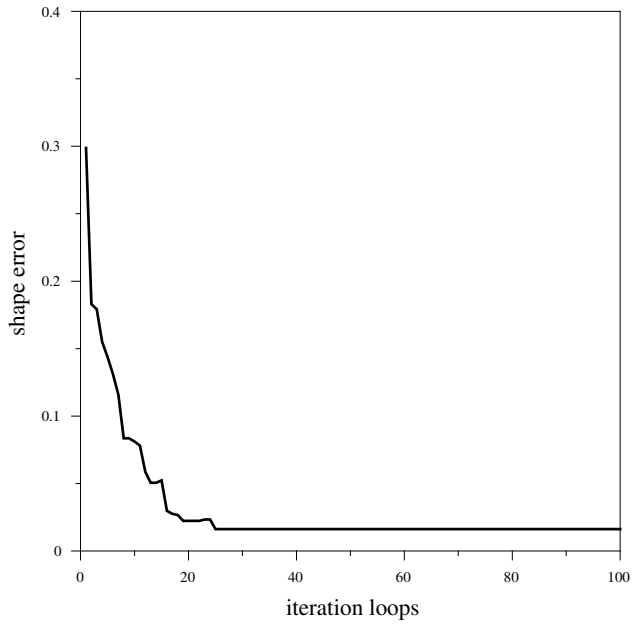


**Figure 5.** The shape error with respective to iteration loops for the first example.

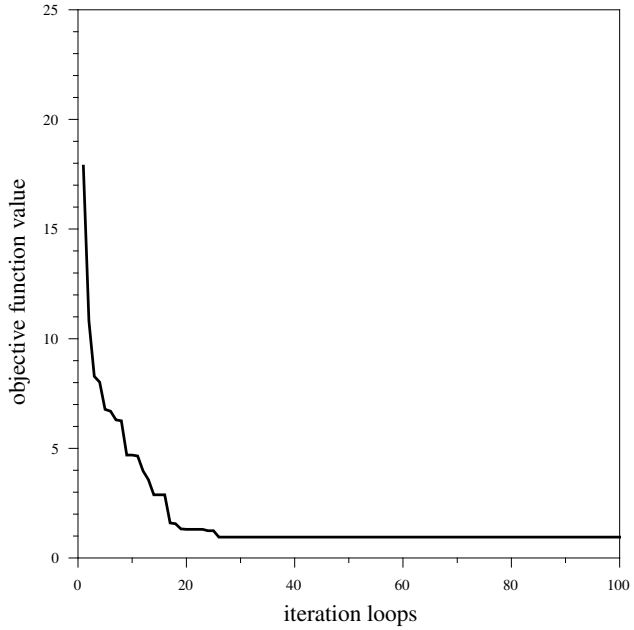


**Figure 6.** The objective function value with respective to iteration loops for the first example.

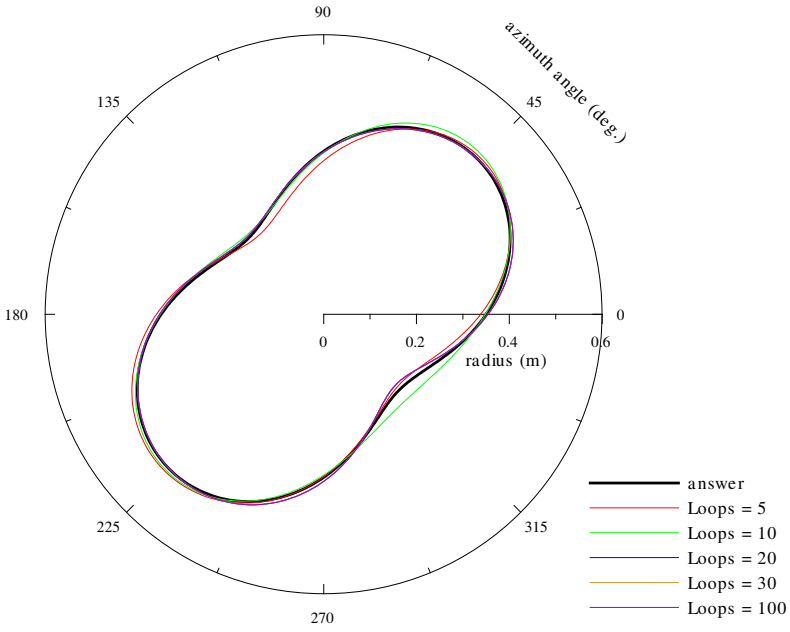


**Figure 7.** The reconstructed target shape of the second example.

shows the objective function value with respective to iteration loops. Fig. 4 to Fig. 6 show that the reconstructed target shape is in good agreement with the true (answer) target shape. In addition, they also show that the inverse scattering scheme based on our modified fireworks algorithm converges very fast.

Note that the target shape of the previous example is convex so that there is no multiple scattering effect. In the second example, the target shape function is given as $h(\phi) = 0.35 + 0.12\sin(2\phi)$, which is slightly concave as shown in Fig. 7. The other conditions are the same as those of the first example. Following the above inverse scattering procedures, the reconstructed target shape of different iteration

loops is plotted in Fig. 7. Fig. 8 shows the shape error with respective to iteration loops. Fig. 9 shows the objective function value with respective to iteration loops. Fig. 7 to Fig. 9 show that the reconstructed target shape is in good agreement with the true (answer) target shape. In addition, they also show that the inverse scattering scheme based on our modified fireworks algorithm converges very fast. Since the target shape of this example is slightly concave, our inverse scattering scheme can tolerate slight multiple scattering.

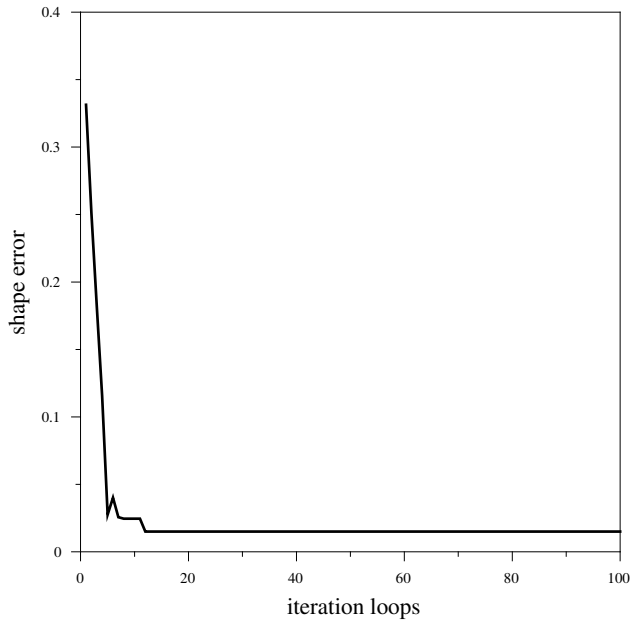


**Figure 8.** The shape error with respective to iteration loops for the second example.

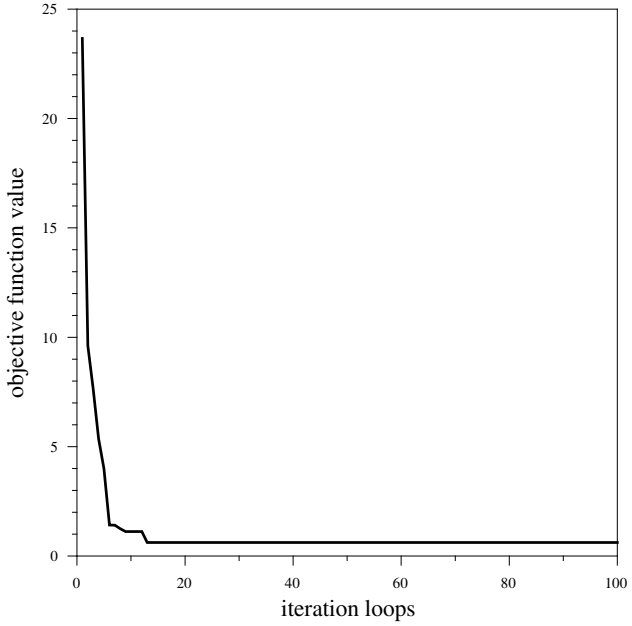


**Figure 9.** The objective function value with respective to iteration loops for the second example.

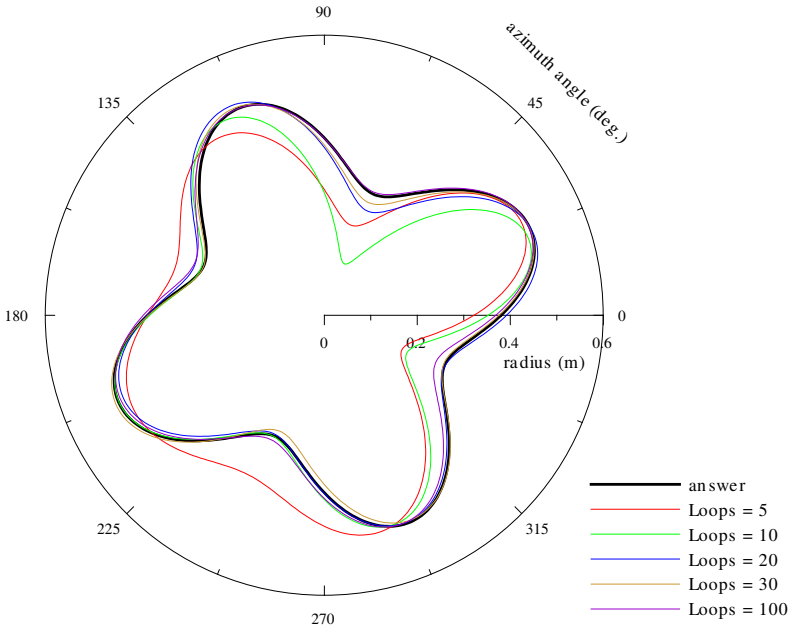


**Figure 10.** The reconstructed target shape of the third example.

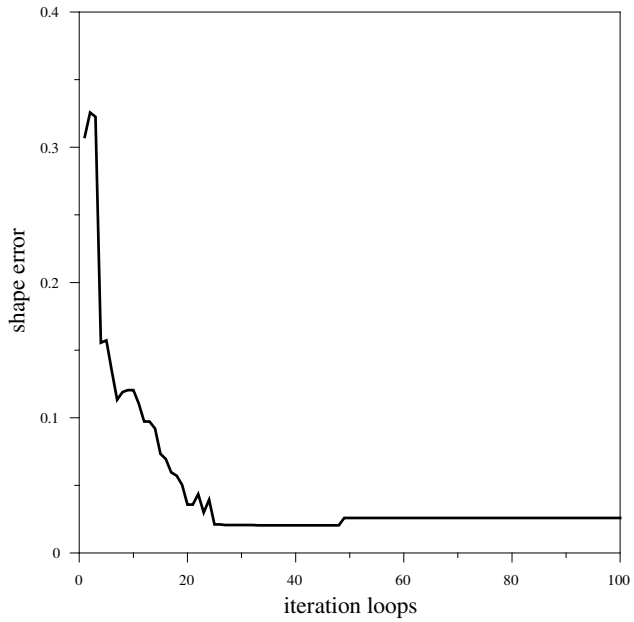


**Figure 11.** The shape error with respective to iteration loops for the third example.

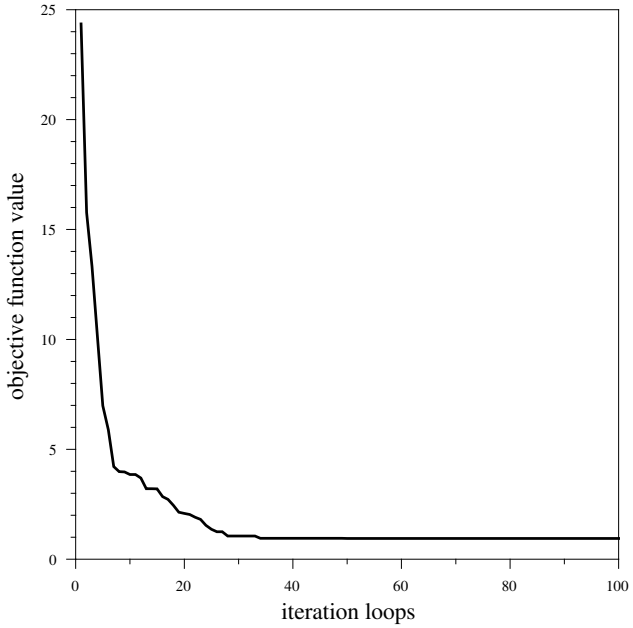


**Figure 12.** The objective function value with respective to iteration loops for the third example.

The shapes of the previous two examples are simple. In the third example, the target shape is given as $h(\phi) = 0.38 + 0.1\sin(4\phi)$. This shape is complex because it contains several concaves, as shown in Fig. 10. The other conditions are the same as those of the previous two examples. Following the above inverse scattering procedures, the reconstructed target shape of different iteration loops is plotted in Fig. 10. Fig. 11 shows the shape error with respective to iteration loops. Fig. 12 shows the objective function value with respective to iteration loops. Fig. 10 to Fig. 12 show that the reconstructed target shape is in good agreement with the true (answer) target shape. They also show that the inverse scattering scheme based on our modified fireworks algorithm converges very fast. Since the target shape of this example contains several concaves, our inverse scattering scheme can tolerate strong multiple scattering mechanisms.

Among all the three examples, the second example has the best converge. This is because both the Fourier series coefficients and the shape of the second example are simple. Based on our modified fireworks algorithm, the target shape can be well predicted within 30 iteration loops, which take about 9 minutes of execution time in personal computer. The above numerical simulation is coded using Fortran programming language together with IMSL library. The hardware is a personal computer with Intel(R) Core(TM) i7-4790 3.6 GHz CPU and 16 GB RAM.

## 6. CONCLUSION

This study successfully combines the moment method solution of scattering integral equations and our modified fireworks algorithm to reconstruct the shape of a conducting cylinder in free space. The inverse scattering problem is first transformed into a nonlinear optimization problem, and then optimized by the modified fireworks algorithm. The fireworks algorithm is a swarm-based optimization algorithm. It does not require any gradient operation. Therefore, the nonlinear characteristic between the input and output may be complex, or even a black box. In addition, the initial guess of each firework location does not affect the overall convergence. This is consistent with our numerical simulation experiences.

There exist many numerical approaches for solving nonlinear optimization problems, e.g., particle swarm algorithms [13], genetic algorithms [21], and stimulated annealing algorithms [22]. In [12], the fireworks algorithm has been proved to converge faster than the particle swarm algorithm. The genetic algorithm implements optimization by binary searching. The fireworks algorithm converges faster than

the genetic algorithm because transformations between decimal and binary systems are not required. As mentioned in Section 4, the fireworks algorithm considers both the good (dense) and bad (sparse) fireworks. It has less chance to get stuck in local optima than the simulated annealing algorithm. With the use of our modified fireworks algorithm, the reconstructed target shape is accurate, and the convergence is fast. In general, a nonlinear electromagnetic problem can be characterized by $f(\bar{x}) = 0$, where $f(\cdot)$ is a nonlinear function, and $\bar{x}$ is a vector composed of all variables. According to the idea of this study, it can be transformed into another optimization problem, which is to search an optimal $\bar{x}$ minimizing $|f(\bar{x})|$. Therefore, the fireworks algorithm based procedures of this study can also be applied to many other nonlinear electromagnetic problems, e.g., nonlinear antennas [21].

## ACKNOWLEDGMENT

The author would like to acknowledge the financial support of the Ministry of Science and Technology, Taiwan, under contract number of MOST 106-2221-E-006-117. The author is also grateful to Mr. Jhong-Yuan Wang, Master of Science in National Cheng-Kung University, Taiwan for his helpful discussion.

## REFERENCES

1. Lewis, R. M., "Physical optics inverse diffraction," *IEEE Transactions on Antennas and Propagation*, Vol. 17, 308–314, 1969.
2. Farhat, N. H., T. Dzekov, and E. Ledet, "Computer simulation of frequency swept imaging," *Proceedings of the IEEE*, Vol. 64, 1453–1454, 1976.
3. Chi, C. and N. H. Farhat, "Frequency swept tomographic imaging of three-dimensional perfectly conducting objects," *IEEE Transactions on Antennas and Propagation*, Vol. 29, 312–319, 1981.
4. Bojarski, N. N., "A survey of the physical optics inverse scattering identity," *IEEE Transaction on Antennas and Propagation*, Vol. 30, 980–989, 1982.
5. Ge, D. B., "A study of the Lewis method for target-shape reconstruction," *Inverse Problems*, Vol. 6, 363–370, 1990.
6. Roger, A., "Newton-Kantorovitch algorithm applied to an electromagnetic inverse problem," *IEEE Transactions on Antennas and Propagation*, Vol. 29, 980–989, 1981.
7. Kirsch, A., R. Kress, P. Monk, and A. Zinn, "Two methods for solving the inverse acoustic scattering problem," *Inverse Problems*, Vol. 4, 749–770, 1988.
8. Colton, D. and P. Monk, "A new method for solving the inverse scattering problem for acoustic waves in an inhomogeneous medium," *Inverse Problems*, Vol. 5, 1013–1026, 1989.
9. Otto, G. P. and W. C. Chew, "Microwave inverse scattering-local shape function imaging for improved resolution of strong scatterers," *IEEE Transactions on Microwave Theory and Techniques*, Vol. 42, 137–141, 1994.
10. Hettlich, F., "Two method for solving an inverse conductive scattering problem," *Inverse Problems*, Vol. 10, 375–385, 1994.
11. Chiu, C. C. and P. T. Liu, "Image reconstruction of a perfectly conducting cylinder by the genetic algorithm," *IEE Proceedings — Microwaves, Antennas and Propagation*, Vol. 143, 259–253, 1996.
12. Tan, Y. and Y. Zhu, "Fireworks algorithm for optimization," *International Conference on Swarm Intelligence (ICSI'2010)*, Beijing, China, June 12–15, 2010.
13. Robinson, J. and Y. Rahmat-Samii, "Particle swarm optimization in electromagnetics," *IEEE Transactions on Antennas and Propagation*, Vol. 52, 397–407, 2004.
14. Balanis, C. A., *Advanced Engineering Electromagnetics*, Wiley, NY, 1989.
15. Harrington, R. F., *Field Computation by Moment Methods*, Macmillan, NY, 1968.
16. Oppenheim, A. V., R. W. Schafer, and J. R. Buck, *Discrete-time Signal Processing*, Prentice Hall, NJ, 1999.
17. Bartels, R. H., J. C. Beatty, and B. A. Barsky, *Hermite and Cubic Spline Interpolation*, Morgan Kaufmann, CA, 1998.

18. Rocca, P. and A. F. Morabito, "Optimal synthesis of reconfigurable planar arrays with simplified architectures for monopulse radar applications," *IEEE Transactions on Antennas and Propagation*, Vol. 63, 1048–1058, 2015.
19. Catapano, I., L. Di Donato, L. Crocco, O. M. Bucci, A. F. Morabito, T. Isernia, and R. Massa, "On quantitative microwave tomography of female breast," *Progress In Electromagnetics Research*, Vol. 97, 75–93, 2009.
20. Bucci, O. M. and G. Franceschetti, "On the degrees of freedom of scattered fields," *IEEE Transactions on Antennas and Propagation*, Vol. 37, 918–926, 1989.
21. Lee, K. C., "Genetic algorithms based analyses of nonlinearly loaded antenna arrays including mutual coupling effects, *IEEE Transactions on Antennas and Propagation*, Vol. 51, 776–781, 2003.
22. Kirkpatrick, S., C. D. Gelatt Jr., and M. P. Vecchi, "Optimization by simulated annealing," *Science*, Vol. 220, 671–680, 1983.